

to appear in *Time-Frequency Signal Analysis and Processing*,
B. Boashash, Ed., Englewood Cliffs (NJ): Prentice Hall, 2002.

CONTENTS

12.4 Time-Frequency Methods for Statistical Signal Processing (F. Hlawatsch and G. Matz)	2
12.4.1 Nonstationary Signal Estimation	2
12.4.2 Nonstationary Signal Detection	5
12.4.3 Summary and Conclusions	9

12.4 TIME-FREQUENCY METHODS FOR NONSTATIONARY STATISTICAL SIGNAL PROCESSING⁰

In this article, we will use the generalized Wigner-Ville spectrum (GWVS) and the generalized Weyl symbol (GWS) to develop time-frequency (TF) techniques for the estimation and detection of underspread nonstationary processes. These TF techniques extend optimal signal estimators (Wiener filters) and optimal signal detectors for the stationary case to underspread nonstationary processes. They are conceptually simple and intuitively appealing as well as computationally efficient and stable.

We will first review some fundamentals (for more details see Articles 4.7 and 9.4). The GWVS of a nonstationary random process $x(t)$ with correlation function $r_x(t, t') = E\{x(t)x^*(t')\}$ is defined as

$$\overline{W}_x^{(\alpha)}(t, f) \triangleq \int_{-\infty}^{\infty} r_x\left(t + \left(\frac{1}{2} - \alpha\right)\tau, t - \left(\frac{1}{2} + \alpha\right)\tau\right) e^{-j2\pi f\tau} d\tau, \quad (12.4.1)$$

where α is a real-valued parameter. The GWS of a linear, time-varying (LTV) system \mathbf{H} with kernel (impulse response) $h(t, t')$ is defined as

$$L_{\mathbf{H}}^{(\alpha)}(t, f) \triangleq \int_{-\infty}^{\infty} h\left(t + \left(\frac{1}{2} - \alpha\right)\tau, t - \left(\frac{1}{2} + \alpha\right)\tau\right) e^{-j2\pi f\tau} d\tau.$$

In the case of a stationary process, the GWVS reduces to the conventional power spectral density. Similarly, for a linear, time-invariant (LTI) system, the GWS reduces to the conventional transfer function (frequency response).

A nonstationary process $x(t)$ is said to be *underspread* if components of $x(t)$ that are sufficiently separated in the TF plane are effectively uncorrelated (see Article 9.4). Two random processes $x(t)$, $y(t)$ are said to be *jointly underspread* if they satisfy similar underspread conditions [4]. An LTV system \mathbf{H} is said to be underspread if it produces only small TF displacements of the input signal (see Article 4.7).

12.4.1 Nonstationary Signal Estimation

The enhancement or estimation of signals corrupted by noise or other interference is important in many signal processing applications. Here, we consider estimation of a nonstationary, zero-mean random signal $s(t)$ from a noise-corrupted observed signal $x(t) = s(t) + n(t)$ by means of an LTV system \mathbf{H} . The signal estimate is thus given by

$$\hat{s}(t) = (\mathbf{H}x)(t) = \int_{-\infty}^{\infty} h(t, t') x(t') dt'. \quad (12.4.2)$$

⁰Authors: **F. Hlawatsch** and **G. Matz**, Institute of Communications and Radio-Frequency Engineering, Vienna University of Technology, Gusshausstrasse 25/389, A-1040 Vienna, Austria (email: fhlawats@pop.tuwien.ac.at, g.matz@ieee.org, web: <http://www.nt.tuwien.ac.at/dspgroup/time.html>). Reviewers: P. Flandrin and S. Carstens-Behrens. This work was supported by FWF grant P11904-TEC.

The additive noise $n(t)$ is nonstationary and assumed uncorrelated with $s(t)$.

The time-varying Wiener filter. The LTV system \mathbf{H} that minimizes the mean-square error (MSE) $\mathbb{E}\{\|\hat{s} - s\|^2\}$ is the *time-varying Wiener filter* [14] [17]

$$\mathbf{H}_W = \mathbf{R}_s(\mathbf{R}_s + \mathbf{R}_n)^{-1}. \quad (12.4.3)$$

Here, \mathbf{R}_s and \mathbf{R}_n denote the correlation operators¹ of signal and noise, respectively. For stationary random processes, \mathbf{H}_W is an LTI system whose frequency response is given by [14] [17]

$$H_W(f) = \frac{P_s(f)}{P_s(f) + P_n(f)}, \quad (12.4.4)$$

where $P_s(f)$ and $P_n(f)$ denote the power spectral density of signal and noise, respectively. This frequency-domain expression involves merely a product and a reciprocal of functions (instead of a product and an inverse of operators as in (12.4.3)) and thus allows a simple design and interpretation of time-invariant Wiener filters.

TF formulation of time-varying Wiener filters. We may ask whether a simple formulation similar to (12.4.4) can be obtained for the time-varying Wiener filter \mathbf{H}_W by replacing $H_W(f)$ with the GWS $L_{\mathbf{H}_W}^{(\alpha)}(t, f)$ and $P_s(f)$, $P_n(f)$ with the GWVS $\overline{W}_s^{(\alpha)}(t, f)$, $\overline{W}_n^{(\alpha)}(t, f)$. Indeed, for *jointly underspread* processes $s(t)$ and $n(t)$, it can be shown [4] that the time-varying Wiener filter \mathbf{H}_W can be written as the sum of two components: (i) an overspread (i.e., not underspread) system component that has negligible effect on the system's performance (MSE) and thus can be disregarded, and (ii) an underspread system component, hereafter denoted as \mathbf{H}_W^u , that allows the approximate TF formulation

$$L_{\mathbf{H}_W^u}^{(\alpha)}(t, f) \approx \frac{\overline{W}_s^{(\alpha)}(t, f)}{\overline{W}_s^{(\alpha)}(t, f) + \overline{W}_n^{(\alpha)}(t, f)}. \quad (12.4.5)$$

This TF formulation extends (12.4.4) to the underspread nonstationary case and allows a simple and intuitively appealing TF interpretation of the time-varying Wiener filter (see Fig. 12.1). Let \mathcal{R}_s and \mathcal{R}_n denote the effective support regions of $\overline{W}_s^{(\alpha)}(t, f)$ and $\overline{W}_n^{(\alpha)}(t, f)$, respectively. In the “signal only” TF region $\mathcal{R}_s \setminus \mathcal{R}_n$, (12.4.5) gives $L_{\mathbf{H}_W^u}^{(\alpha)}(t, f) \approx 1$. Thus, \mathbf{H}_W^u passes all “noise-free” components of $x(t)$ without attenuation or distortion. In the “noise only” TF region $\mathcal{R}_n \setminus \mathcal{R}_s$, (12.4.5) gives $L_{\mathbf{H}_W^u}^{(\alpha)}(t, f) \approx 0$, i.e., \mathbf{H}_W^u suppresses all components of $x(t)$ located in TF regions where there is no signal. Finally, in the “signal plus noise” TF region $\mathcal{R}_s \cap \mathcal{R}_n$, $|L_{\mathbf{H}_W^u}^{(\alpha)}(t, f)|$ assumes values approximately between 0 and 1. Here, \mathbf{H}_W^u performs an attenuation that depends on the signal-to-noise ratio at the respective TF point.

¹The correlation operator \mathbf{R}_x of a nonstationary random process $x(t)$ is the positive (semi-) definite linear operator whose kernel equals the correlation function $r_x(t, t') = \mathbb{E}\{x(t)x^*(t')\}$.

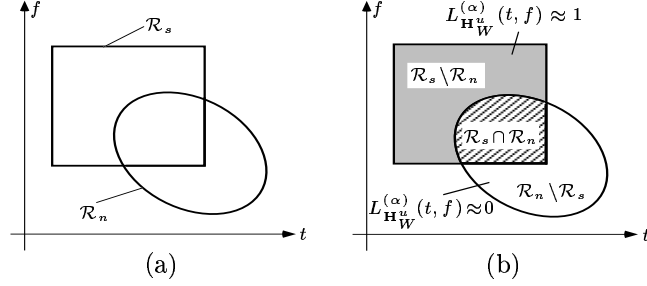


Figure 12.1: TF interpretation of the time-varying Wiener filter \mathbf{H}_W for jointly underspread signal and noise processes: (a) Effective TF support regions of signal and noise, (b) TF pass, stop, and transition regions of the time-varying Wiener filter.

TF design of time-varying Wiener filters. The TF formulation (12.4.5) suggests a simple *TF design* of nonstationary signal estimators. Let us define the “TF pseudo-Wiener filter” $\tilde{\mathbf{H}}_W$ by setting its GWS equal to the right-hand side of (12.4.5) [4]:

$$L_{\tilde{\mathbf{H}}_W}^{(\alpha)}(t, f) \triangleq \frac{\overline{W}_s^{(\alpha)}(t, f)}{\overline{W}_s^{(\alpha)}(t, f) + \overline{W}_n^{(\alpha)}(t, f)}. \quad (12.4.6)$$

For jointly underspread processes $s(t)$, $n(t)$ where (12.4.5) is a good approximation, the TF pseudo-Wiener filter $\tilde{\mathbf{H}}_W$ will closely approximate (the underspread part of) the optimal Wiener filter \mathbf{H}_W ; furthermore, it can be shown that $\tilde{\mathbf{H}}_W$ will then be nearly independent of the value of α used in (12.4.6). For processes $s(t)$, $n(t)$ that are *not* jointly underspread, however, $\tilde{\mathbf{H}}_W$ must be expected to perform poorly.

Whereas the TF pseudo-Wiener filter $\tilde{\mathbf{H}}_W$ is *designed* in the TF domain, the calculation of the signal estimate $\hat{s}(t)$ can be performed in the time domain according to (12.4.2). The impulse response of $\tilde{\mathbf{H}}_W$ is obtained from $L_{\tilde{\mathbf{H}}_W}^{(\alpha)}(t, f)$ as (cf. Article 4.7)

$$\tilde{h}_W(t, t') = \int_{-\infty}^{\infty} L_{\tilde{\mathbf{H}}_W}^{(\alpha)}\left(\left(\frac{1}{2} + \alpha\right)t + \left(\frac{1}{2} - \alpha\right)t', f\right) e^{j2\pi f(t-t')} df. \quad (12.4.7)$$

An efficient implementation of the TF pseudo-Wiener filter $\tilde{\mathbf{H}}_W$ that is based on the multiwindow short-time Fourier transform is discussed in [4] [7].

Compared to the Wiener filter \mathbf{H}_W , the TF pseudo-Wiener filter $\tilde{\mathbf{H}}_W$ possesses two practical advantages. First, the prior knowledge required for calculating $\tilde{\mathbf{H}}_W$ is given by the GWVS $\overline{W}_s^{(\alpha)}(t, f)$ and $\overline{W}_n^{(\alpha)}(t, f)$ that are more intuitive and easier to handle than the correlation operators \mathbf{R}_s and \mathbf{R}_n . Second, the TF design (12.4.6) is less computationally intensive and more stable than (12.4.3) since it requires pointwise (scalar) divisions of functions instead of operator inversions.

Robust TF Wiener filters. The performance of the filters \mathbf{H}_W and $\tilde{\mathbf{H}}_W$ is sensitive to deviations of the second-order statistics (correlations or GWVS) from the nominal

statistics for which these filters were designed. This motivates the use of *minimax robust Wiener filters* that optimize the worst-case performance (maximum MSE) within specified uncertainty classes of second-order statistics [11] [12].

Consider a partition of the TF plane into K mutually disjoint TF regions \mathcal{R}_i , $i = 1, \dots, K$. Extending the stationary case definition in [5], we define so-called *p-point uncertainty classes* \mathcal{S} and \mathcal{N} as the sets of all nonnegative TF functions (not necessarily valid GWVS) $\widetilde{W}_s(t, f)$ and $\widetilde{W}_n(t, f)$ that have prescribed energies s_i and n_i , respectively, within \mathcal{R}_i , i.e., $\iint_{\mathcal{R}_i} \widetilde{W}_s(t, f) dt df = s_i$ and $\iint_{\mathcal{R}_i} \widetilde{W}_n(t, f) dt df = n_i$ for $i = 1, \dots, K$. For these uncertainty classes, the GWS of the *minimax robust TF Wiener filter* \mathbf{H}_R is given by [11] [12]

$$L_{\mathbf{H}_R}^{(\alpha)}(t, f) = \sum_{i=1}^K \frac{s_i}{s_i + n_i} I_{\mathcal{R}_i}(t, f), \quad (12.4.8)$$

where $I_{\mathcal{R}_i}(t, f)$ is the indicator function of \mathcal{R}_i (i.e., $I_{\mathcal{R}_i}(t, f)$ is 1 for (t, f) inside \mathcal{R}_i and 0 outside \mathcal{R}_i). Note that $L_{\mathbf{H}_R}^{(\alpha)}(t, f)$ is piecewise constant, expressing constant TF weighting within \mathcal{R}_i . The performance of \mathbf{H}_R is approximately independent of the actual second-order statistics as long as they are within \mathcal{S} , \mathcal{N} [11] [12]. Signal-adaptive, online implementations of robust time-varying Wiener filters using local cosine bases have been proposed in [12] [13].

Simulation results. Fig. 12.2(a), (b) shows the Wigner-Ville spectra (GWVS with $\alpha = 0$) of jointly underspread signal and noise processes. The Weyl symbols (GWS with $\alpha = 0$) of the corresponding Wiener filter \mathbf{H}_W , of its underspread part \mathbf{H}_W^u , and of the TF pseudo-Wiener filter $\widetilde{\mathbf{H}}_W$ are shown in Fig. 12.2(c)–(e). It is verified that the Weyl symbol of $\widetilde{\mathbf{H}}_W$ approximates that of \mathbf{H}_W^u . The mean SNR improvement achieved by the TF pseudo-Wiener filter $\widetilde{\mathbf{H}}_W$ was obtained as 6.11 dB; this is nearly as good as that of the Wiener filter \mathbf{H}_W (6.14 dB).

To illustrate the performance of the robust TF Wiener filter \mathbf{H}_R , we used $K = 4$ rectangular TF regions \mathcal{R}_i to define *p-point uncertainty classes* \mathcal{S} and \mathcal{N} as described above. The regional energies s_i and n_i were obtained by integrating the nominal Wigner-Ville spectra in Fig. 12.2(a), (b) over the TF regions \mathcal{R}_i . The Weyl symbol of the robust TF Wiener filter \mathbf{H}_R in (12.4.8) is shown in Fig. 12.2(f). Fig. 12.3 compares the nominal and worst-case performance of the Wiener filter \mathbf{H}_W (designed for the nominal Wigner-Ville spectra in Fig. 12.2(a), (b)) with the performance of the robust TF Wiener filter \mathbf{H}_R . It is seen that \mathbf{H}_R achieves a substantial performance improvement over \mathbf{H}_W at worst-case operating conditions with only a slight performance loss at nominal operating conditions.

12.4.2 Nonstationary Signal Detection

Next, we consider the discrimination of two nonstationary, zero-mean, Gaussian random signals $x_0(t)$ and $x_1(t)$. The hypotheses are

$$H_0 : x(t) = x_0(t) \quad \text{vs.} \quad H_1 : x(t) = x_1(t).$$

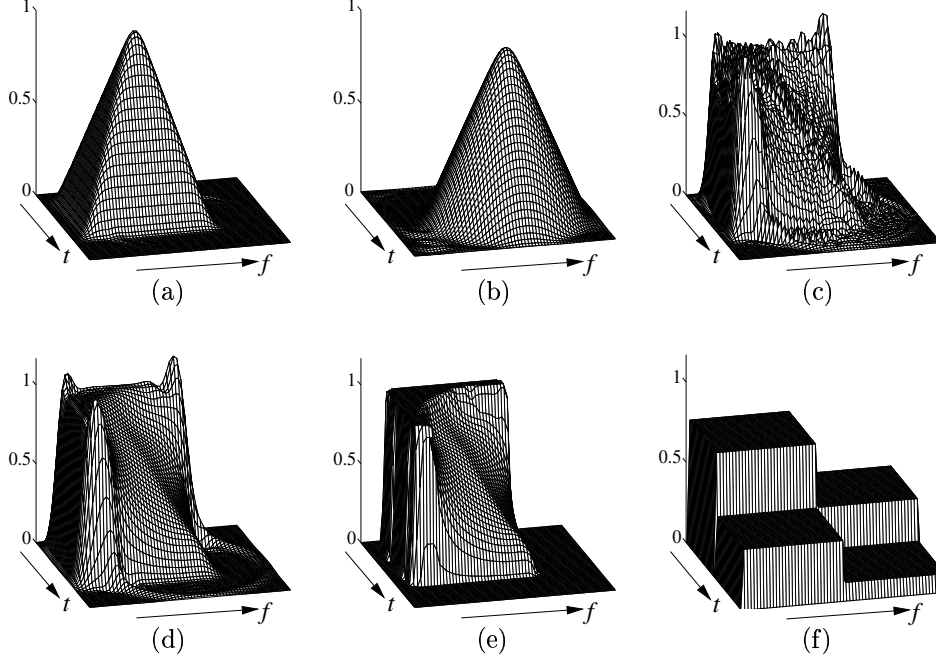


Figure 12.2: TF representations of signal and noise statistics and of various Wiener-type filters: (a) Wigner-Ville spectrum of $s(t)$, (b) Wigner-Ville spectrum of $n(t)$, (c) Weyl symbol of Wiener filter \mathbf{H}_W , (d) Weyl symbol of underspread part \mathbf{H}_W^u of \mathbf{H}_W , (e) Weyl symbol of TF pseudo-Wiener filter $\tilde{\mathbf{H}}_W$, (f) Weyl symbol of robust TF Wiener filter \mathbf{H}_R . The time duration is 128 samples; normalized frequency ranges from $-1/4$ to $1/4$.

The optimal detector. The optimal likelihood ratio detector [14] [17] calculates a quadratic form of the observed signal $x(t)$,

$$\Lambda(x) = \langle \mathbf{H}_L x, x \rangle = \int_{-\infty}^{\infty} \int_{-\infty}^{\infty} h_L(t, t') x(t') x^*(t) dt dt', \quad (12.4.9)$$

with the operator (LTV system) \mathbf{H}_L given by

$$\mathbf{H}_L = \mathbf{R}_{x_0}^{-1} - \mathbf{R}_{x_1}^{-1} = \mathbf{R}_{x_0}^{-1}(\mathbf{R}_{x_1} - \mathbf{R}_{x_0})\mathbf{R}_{x_1}^{-1}. \quad (12.4.10)$$

The test statistic $\Lambda(x)$ is then compared to a threshold to decide whether H_0 or H_1 is in force. For stationary processes, $\Lambda(x)$ can be expressed in terms of the Fourier transform $X(f)$ of $x(t)$ and the power spectral densities of $x_0(t)$ and $x_1(t)$ as

$$\Lambda(x) = \int_{-\infty}^{\infty} |X(f)|^2 H_L(f) df, \quad \text{with } H_L(f) = \frac{P_{x_1}(f) - P_{x_0}(f)}{P_{x_0}(f) P_{x_1}(f)}. \quad (12.4.11)$$

This frequency-domain expression involves simple products and reciprocals of functions (instead of operator products and inverses as in (12.4.10)) and thus allows a

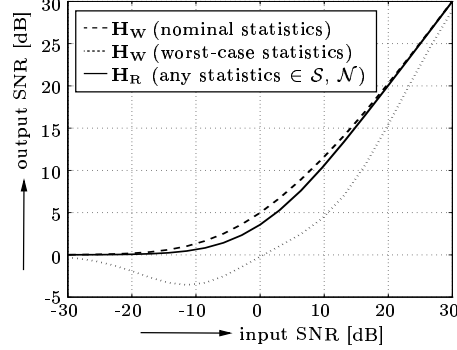


Figure 12.3: Comparison of the performance (output SNR vs. input SNR) of the ordinary Wiener filter \mathbf{H}_W and the robust TF Wiener filter \mathbf{H}_R for various operating conditions.

simple interpretation and design of likelihood ratio detectors in the stationary case.

TF formulation of nonstationary detectors. It is known [2] that the quadratic test statistic in (12.4.9) can be rewritten as

$$\Lambda(x) = \int_{-\infty}^{\infty} \int_{-\infty}^{\infty} W_x^{(\alpha)}(t, f) L_{\mathbf{H}_L}^{(\alpha)*}(t, f) dt df, \quad (12.4.12)$$

where

$$W_x^{(\alpha)}(t, f) = \int_{-\infty}^{\infty} x\left(t + \left(\frac{1}{2} - \alpha\right)\tau\right) x^*\left(t - \left(\frac{1}{2} + \alpha\right)\tau\right) e^{-j2\pi f\tau} d\tau$$

is the generalized Wigner distribution [3] of the observed signal $x(t)$. Thus, $\Lambda(x)$ can be interpreted as a weighted integral of $W_x^{(\alpha)}(t, f)$, with the TF weight function being the conjugate of the GWS of the operator \mathbf{H}_L .

In analogy to Section 12.4.1, a simplified approximate TF formulation of $\Lambda(x)$ exists for *jointly underspread* processes $x_0(t)$, $x_1(t)$. Here, the operator \mathbf{H}_L can be written as the sum of an overspread component whose effect is negligible and an underspread component, denoted \mathbf{H}_L^u , whose GWS can be approximated as [8]

$$L_{\mathbf{H}_L^u}^{(\alpha)}(t, f) \approx \frac{\overline{W}_{x_1}^{(\alpha)}(t, f) - \overline{W}_{x_0}^{(\alpha)}(t, f)}{\overline{W}_{x_0}^{(\alpha)}(t, f) \overline{W}_{x_1}^{(\alpha)}(t, f)}. \quad (12.4.13)$$

Substituting this approximation of $L_{\mathbf{H}_L^u}^{(\alpha)}(t, f)$ for $L_{\mathbf{H}_L}^{(\alpha)}(t, f)$ in (12.4.12), we obtain the following approximate TF formulation of our test statistic,

$$\Lambda(x) \approx \int_{-\infty}^{\infty} \int_{-\infty}^{\infty} W_x^{(\alpha)}(t, f) \left[\frac{\overline{W}_{x_1}^{(\alpha)}(t, f) - \overline{W}_{x_0}^{(\alpha)}(t, f)}{\overline{W}_{x_0}^{(\alpha)}(t, f) \overline{W}_{x_1}^{(\alpha)}(t, f)} \right]^* dt df. \quad (12.4.14)$$

This TF formulation extends (12.4.11) to the underspread nonstationary case and allows an intuitively appealing TF interpretation that is analogous to the one given

in Section 12.4.1 in the context of the approximation (12.4.5).

TF design of nonstationary detectors. The TF formulation (12.4.14) suggests a simple *TF design* of nonstationary detectors. In analogy to (12.4.12), we define the test statistic

$$\tilde{\Lambda}(x) \triangleq \int_{-\infty}^{\infty} \int_{-\infty}^{\infty} W_x^{(\alpha)}(t, f) L_{\tilde{\mathbf{H}}_L}^{(\alpha)*}(t, f) dt df,$$

where the operator (LTV system) $\tilde{\mathbf{H}}_L$ is defined by setting its GWS equal to the right-hand side of (12.4.13) [8]:

$$L_{\tilde{\mathbf{H}}_L}^{(\alpha)}(t, f) \triangleq \frac{\overline{W}_{x_1}^{(\alpha)}(t, f) - \overline{W}_{x_0}^{(\alpha)}(t, f)}{\overline{W}_{x_0}^{(\alpha)}(t, f) \overline{W}_{x_1}^{(\alpha)}(t, f)}.$$

For jointly underspread processes $x_0(t)$, $x_1(t)$ where (12.4.13) is a good approximation, $\tilde{\mathbf{H}}_L$ will closely approximate (the underspread part of) \mathbf{H}_L , and thus the performance of the TF designed detector $\tilde{\Lambda}(x)$ will be similar to that of the optimal likelihood ratio detector $\Lambda(x)$. For processes $x_0(t)$, $x_1(t)$ that are *not* jointly underspread, however, $\tilde{\Lambda}(x)$ must be expected to perform poorly.

Whereas the detector $\tilde{\Lambda}(x)$ is designed in the TF domain, it can be implemented in the time domain in complete analogy to (12.4.9). The impulse response $\tilde{h}_L(t, t')$ of $\tilde{\mathbf{H}}_L$ can be obtained from $L_{\tilde{\mathbf{H}}_L}^{(\alpha)}(t, f)$ by an inverse Weyl transformation (cf. (12.4.7)).

An efficient implementation of the TF detector $\tilde{\Lambda}(x)$ that uses the multiwindow short-time Fourier transform is discussed in [9].

Compared to the likelihood ratio detector $\Lambda(x)$, the TF designed detector $\tilde{\Lambda}(x)$ is practically advantageous because the statistical *a priori* knowledge required for its design is formulated in the intuitively accessible TF domain, and because its design is less computationally intensive and more stable since operator inversions are replaced by pointwise divisions of functions. These advantages are analogous to the advantages of the TF pseudo-Wiener filter discussed in Section 12.4.1.

Simulation results. We first consider $x_0(t) = n(t)$ and $x_1(t) = s(t) + n(t)$, where signal $s(t)$ and noise $n(t)$ are jointly underspread, uncorrelated, zero-mean, Gaussian processes with Wigner-Ville spectra as shown in Fig. 12.4(a), (b). From Fig. 12.4(c), (d), we verify that the Weyl symbols of the optimal operator \mathbf{H}_L and the TF designed operator $\tilde{\mathbf{H}}_L$ are effectively identical. Also, Fig. 12.4(e), (f) shows that the performance of the TF designed detector $\tilde{\Lambda}(x)$ closely approximates that of the likelihood ratio detector $\Lambda(x)$.

Our next example concerns the detection of knocking combustions in car engines (see Article 15.2 and refs. [1] [9] [10] for background and details). Here, $x_0(t)$ is the nonknocking signal and $x_1(t)$ is the knocking signal. Estimates of the correlations of $x_0(t)$ and $x_1(t)$ were computed from a set of labeled training data,² and estimates

²We are grateful to S. Carstens-Behrens, M. Wagner, and J. F. Böhme for illuminating discussions and for providing us with the labeled car engine data.

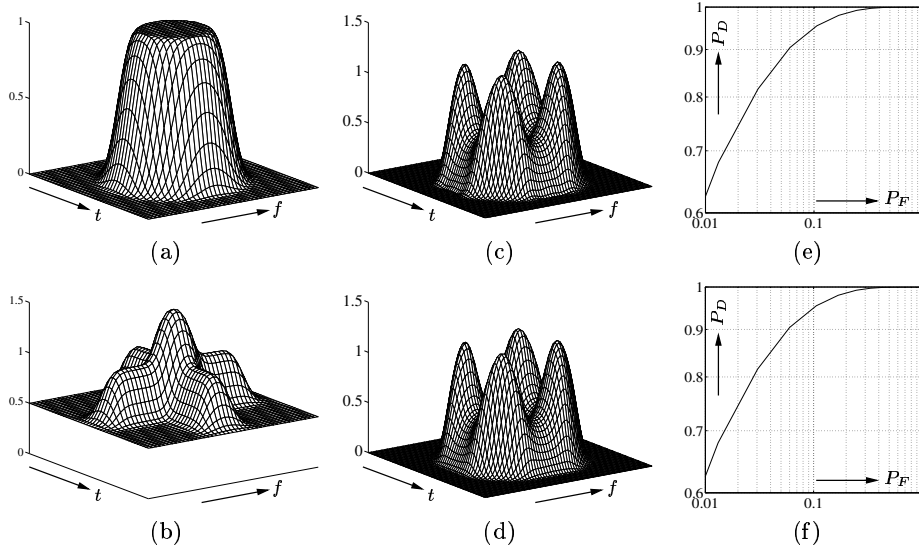


Figure 12.4: Comparison of likelihood ratio detector $\Lambda(x)$ and TF designed detector $\tilde{\Lambda}(x)$: (a) Wigner-Ville spectrum of $s(t)$, (b) Wigner-Ville spectrum of $n(t)$, (c) Weyl symbol of \mathbf{H}_L , (d) Weyl symbol of $\tilde{\mathbf{H}}_L$, (e) receiver operator characteristics (ROC) [14] of $\Lambda(x)$, (f) ROC of $\tilde{\Lambda}(x)$. The ROCs were obtained by Monte Carlo simulation. The time duration is 128 samples; normalized frequency ranges from $-1/4$ to $1/4$.

of the Wigner-Ville spectra (shown in Fig. 12.5(a), (b)) were derived according to (12.4.1). The likelihood ratio detector $\Lambda(x)$ and the TF designed detector $\tilde{\Lambda}(x)$ were constructed using these estimated statistics, and the performance of these detectors was analyzed by applying them to a different set of labeled data. It can be seen from Fig. 12.5(c) that the TF designed detector performs significantly better than the theoretically optimal likelihood ratio detector. This is due to numerical problems that occurred in the design of the likelihood ratio detector. Specifically, the estimated correlation matrices³ were poorly conditioned. Despite the use of pseudo-inverses, the inversion of these matrices (which is required for the design of the likelihood ratio detector) could not be stabilized sufficiently. In contrast, the design of the TF detector merely involves a pointwise division of the estimated Wigner-Ville spectra. This is much less affected by numerical problems since divisions by near-to-zero values can easily be stabilized by means of a thresholding.

12.4.3 Summary and Conclusions

The generalized Wigner-Ville spectrum (GWVS) provides a natural extension of the power spectral density to underspread, nonstationary random processes. Similarly, the generalized Weyl symbol (GWS) provides a natural extension of the transfer

³In the discrete-time case, correlation operators are replaced by correlation matrices.

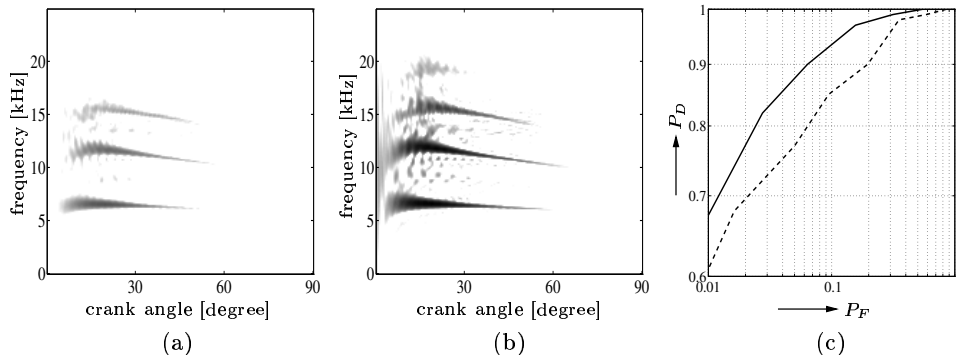


Figure 12.5: Detection of knocking combustions: (a) Estimated Wigner-Ville spectrum of non-knocking combustion process $x_0(t)$, (b) estimated Wigner-Ville spectrum of knocking combustion process $x_1(t)$ (crank angle is proportional to time; signal length is 186 samples), (c) ROCs of likelihood ratio detector $\Lambda(x)$ (dashed line) and TF designed detector $\hat{\Lambda}(x)$ (solid line).

function (frequency response) to underspread, time-varying linear systems. In this article, we have considered the application of the GWVS and GWS to the estimation and detection of underspread, nonstationary random processes. Using the GWVS and GWS, it was possible to extend classical stationary estimators and detectors to the nonstationary case in an intuitive manner. We note that the general approach—replacing the power spectral density with the GWVS and the transfer function with the GWS—is applicable to other problems of statistical signal processing as well, as long as the nonstationary processes involved are (jointly) underspread.

Finally, we note that further time-frequency methods for nonstationary signal estimation and detection are discussed in Articles 8.3, 9.2, 12.1, and 15.2 as well as in refs. [6] [10] [15] [16].

References

- [1] S. Carstens-Behrens, M. Wagner, and J. F. Böhme, “Detection of multiple resonances in noise,” *Int. J. Electron. Commun. (AEÜ)*, vol. 52, no. 5, pp. 285–292, 1998.
- [2] P. Flandrin, “A time-frequency formulation of optimum detection,” *IEEE Trans. Acoust., Speech, Signal Processing*, vol. 36, no. 9, pp. 1377–1384, 1988.
- [3] F. Hlawatsch and P. Flandrin, “The interference structure of the Wigner distribution and related time-frequency signal representations,” in *The Wigner Distribution — Theory and Applications in Signal Processing* (W. Mecklenbräuer and F. Hlawatsch, eds.), pp. 59–133, Amsterdam, The Netherlands: Elsevier, 1997.
- [4] F. Hlawatsch, G. Matz, H. Kirchauer, and W. Kozek, “Time-frequency formulation, design, and implementation of time-varying optimal filters for signal estimation,” *IEEE Trans. Signal Processing*, vol. 48, pp. 1417–1432, May 2000.

- [5] S. A. Kassam and H. V. Poor, "Robust techniques for signal processing: A survey," *Proc. IEEE*, vol. 73, pp. 433–481, March 1985.
- [6] H. A. Khan and L. F. Chaparro, "Nonstationary Wiener filtering based on evolutionary spectral theory," in *Proc. IEEE ICASSP-97*, (Munich, Germany), pp. 3677–3680, May 1997.
- [7] W. Kozek, H. G. Feichtinger, and J. Scharinger, "Matched multiwindow methods for the estimation and filtering of nonstationary processes," in *Proc. IEEE ISCAS-96*, (Atlanta, GA), pp. 509–512, May 1996.
- [8] G. Matz and F. Hlawatsch, "Time-frequency formulation and design of optimal detectors," in *Proc. IEEE-SP Int. Sympos. Time-Frequency Time-Scale Analysis*, (Paris, France), pp. 213–216, June 1996.
- [9] G. Matz and F. Hlawatsch, "Time-frequency methods for signal detection with application to the detection of knock in car engines," in *Proc. IEEE-SP Workshop on Statistical Signal and Array Proc.*, (Portland, OR), pp. 196–199, Sept. 1998.
- [10] G. Matz and F. Hlawatsch, "Time-frequency subspace detectors and application to knock detection," *Int. J. Electron. Commun. (AEÜ)*, vol. 53, no. 6, pp. 379–385, Dec. 1999.
- [11] G. Matz and F. Hlawatsch, "Minimax robust time-frequency filters for nonstationary signal estimation," in *Proc. IEEE ICASSP-99*, (Phoenix, AZ), pp. 1333–1336, March 1999.
- [12] G. Matz and F. Hlawatsch, "Minimax robust nonstationary signal estimation based on a p -point uncertainty model," *J. Franklin Inst.*, vol. 337, pp. 403–419, July 2000.
- [13] G. Matz, F. Hlawatsch, and A. Raidl, "Signal-adaptive robust time-varying Wiener filters: Best subspace selection and statistical analysis," in *Proc. IEEE ICASSP-01*, Salt Lake City (UT), pp. 3945–3948, May 2001.
- [14] H. V. Poor, *An Introduction to Signal Detection and Estimation*. New York: Springer, 1988.
- [15] A. M. Sayeed and D. L. Jones, "Optimal detection using bilinear time-frequency and time-scale representations," *IEEE Trans. Signal Processing*, vol. 43, pp. 2872–2883, Dec. 1995.
- [16] J. A. Sills and E. W. Kamen, "Time-varying matched filters," *Circuits, Systems, Signal Processing*, vol. 15, no. 5, pp. 609–630, 1996.
- [17] H. L. Van Trees, *Detection, Estimation, and Modulation Theory, Part I: Detection, Estimation, and Linear Modulation Theory*. New York: Wiley, 1968.